OPTICAL PRECURSORS IN RUBIDIUM VAPOR AND THEIR RELATION TO SUPERRADIANCE

A Thesis

by

WENLONG YANG

Submitted to the Office of Graduate Studies of
Texas A&M University
in partial fulfillment of the requirements for the degree of

MASTER OF SCIENCE

August 2011

Major Subject: Physics

Optical Precursors in Rubidium Vapor and Their Relation to Superradiance

OPTICAL PRECURSORS IN RUBIDIUM VAPOR AND THEIR RELATION TO SUPERRADIANCE

A Thesis

by

WENLONG YANG

Submitted to the Office of Graduate Studies of
Texas A&M University
in partial fulfillment of the requirements for the degree of

MASTER OF SCIENCE

Approved by:

Chair of Committee,	Alexei V. Sokolov
Committee Members,	Philip R. Hemmer
	George R. Welch
Head of Department,	Edward Fry

August 2011

Major Subject: Physics

ABSTRACT

Optical Precursors in Rubidium Vapor and Their Relation to Superradiance.

(August 2011)

Wenlong Yang, B.S., Nankai University; M.S., Chern Inst. of Math., Nankai University, Tianjin, P. R. China

Chair of Advisory Committee: Dr. Alexei V. Sokolov

Optical precursor is the sharp optical pulse front that does not show delay in absorptive media. In this thesis, optical precursor behavior in rubidium (Rb) vapor was investigated in the picoseconds regime. An amplified femtosecond laser was shaped to a 7-ps square pulse with sharp rising and trailing edges. This pulse was then sent into a hot rubidium vapor, and the center frequency of the laser pulse was absorbed. The output pulses were measured by a fast streak camera with 2-picosecond resolution. By varying the temperature of the Rb vapor, the measured pulse shapes showed the progression of formation of optical precursors. The measured pulses shapes showed good agreement with theory.

On the other hand, a connection between optical precursors and femtosecond laser pumped 3-photon superradiance was investigated in this thesis. Maxwell-Bloch equations were numerically solved in two steps with commercial software Mathematica 8. A good agreement was found between simulation and experiment. It was confirmed that, at low excitation regime, superradiance generated from hot rubidium vapor, which

were pumped by a femtosecond laser, can be understood as the formation of optical precursors.

To my parents

ACKNOWLEDGEMENTS

I would like to thank my committee chair, Dr. Sokolov, for his guidance and support throughout the course of this research. I would like to thank my committee member, Dr. Hemmer, for his teaching of many experiment skills in the beginning of my research. I would like to thank my committee member, Dr. Welch, for sharing some of his personal experiences in scientific research and life. I also want to thank Dr. Kattawar, Dr. Kolomenski, Dr. Strohaber, Dr. Schuessler and Dr. Kalachev for their help, support and encouragement. I also want to thank Dr. Scully for supporting the experiment.

Thanks also go to my friends and colleagues: Gombojav Ariunbold, Xia Hua, Hebin Li, Jiahui Peng, Matthew Springer, Benjamin Stryker, Alexander Sinyukov, Andrew Traverso, Dmitri Voronine, Chao Wang, Kai Wang, Xi Wang, Luqi Yuan, Guowan Zhang, Miaochan Zhi, Feng Zhu, and the department faculty and staff for making my time at Texas A&M University a great experience. I want to thank Dr. Liang, David Huitink, Dr. Ke Wang from mechanical engineering and Dr. Changdong Kim from electronic engineering for their help in the tip sharpening project. I want to thank, specifically, Dr. Huiliang Zhang for teaching me many useful skills and the help in the tip sharpening project. I want to thank Dr. Nevels and Yaqi Lu for their help in the CST simulation. I thank my 2008 classmates for the time we spent together: Zheyang Liao, Jianping Xiao, Kechen Wang, Xiwen Zhang, Jeson Chen, Zhiyuan Wei, Yang Liu, Feng Li, Zhaokai Meng, Wei Zhao, Guangyao Chen. Thanks to my office mates for creating a happy environment in the office: Ellie and Ning Su.

I also want to thank Xin Liu, Huijie Hou, Xiongjun Liu and Leina Zhu for their help in my life and research here, especially when I just arrived in College Station in 2008. I also want to thank Judon and Linda for their care of my family in every possible way. I want to thank friends at Grace Valley Chinese Church for their help. I want to thank friends at Grace Bible Church. I also want to thank our kindly neighbors in Colony Apartments and University Apartments; they make our stay a memorable experience.

I want to thank Dr. Molin Ge for his constant care of my scientific research. I would like to thank my friends in China. Finally, I thank my parents and my relatives for their support and encouragement and my son and my wife for her love.

NOMENCLATURE

fs	femtosecond(s)
FWHM	full width at half maximum
MBE	Maxwell-Bloch Equations
ps	picoseconds(s)
Rb	rubidium

TABLE OF CONTENTS

LIST OF FIGURES

1. INTRODUCTION AND LITERATURE REVIEW

Optical precursor is also called Sommerfeld-Brillouin precursor. Back in 1914, the constancy of speed of light was still challenged by many questions. One of them was whether in dispersive media, where the group velocity of light is larger than the speed of light in vacuum, the propagation of information is still equal to or below the speed of light in vacuum. Arnold Sommerfeld and his student Leon Brillouin discussed this problem and published two papers in 1914 [1, 2]. They considered a pulse with an infinitely sharp front propagating through an absorptive medium and investigated theoretically the speed of propagation of the sharp pulse front. The result was that the pulse front is not delayed and still travels at the speed of light in vacuum and the rest of the pulse is delayed due to the absorption and dispersion. The undelayed pulse front was called optical precursor. Later in Brillouin's book [3], this problem was thoroughly discussed.

Recent rise of interest in optical precursors has several reasons. First of all, with the development of ultrafast laser techniques, optical pulses with rising time of a few femtoseconds are widely available. Therefore, electromagnetic waves with sharp rising edges, which are necessary to generate optical precursors, are easier to obtain. Secondly, the possibility of using an optical precursor as a means of communication medium attracted a lot of attention [4]. Thirdly, also in the above paper [4], the Bouguer–Lambert–Beer(BLB) law, which is a fundamental physical law, was said to be violated

---

This thesis follows the style of Optics Express.

by optical precursors. Research is carried out regarding these issues. Optical precursors have been observed in semiconductor GaAs [5], dielectric absorber [6], and electric induced transparency medium [7, 8]. Our group has clarified that BLB law is not violated when femtosecond pulses propagate in water in linear regime [9]. Recently, the optical precursor behavior has also been observed in an infrared absorber solution [10] in our group. This is the first indication of precursor behavior in the femtosecond regime in bulk medium. Optical precursors have been observed in rubidium vapor for nanosecond pulses through electromagnetic induced transparency [7]. Here in this thesis, we report a direct observation of optical precursor in rubidium vapor in the picoseconds regime.

On the other hand, superradiance is a phenomenon in which the atoms or molecules emit light coherently. As a result, the emitted light has peak intensity orders of magnitude larger than normal spontaneous emission and, at the same time, the time duration of the emission is orders of magnitude shorter than normal spontaneous emission. The theoretical prediction was first made by R. H. Dicke [11]. Many theoretical works were done to consider more and more realistic cases [11-14]. Early experiments were also carried out to show the existence of superradiance in various systems [15, 16]. Two photon excited and 3-photon excited superradiance experiment were also carried out in our group [17, 18].

Superradiance and optical precursor both show oscillations of intensity (ringing) in the pulse shape, they are both due to interaction between light and matter and are governed by the Maxwell-Bloch equations. So it is of interest to investigate the relation between them in rubidium vapor. This thesis is organized like this: in Section 2, the

theoretical calculations and experiment measurements of optical precursor in rubidium vapor are shown; in Section 3, a theoretical explanation of superradiance in rubidium vapor in low excitation regime is given, and the connection between superradiance and optical precursor is discussed; conclusions are given in Section 4.

2. OPTICAL PRECURSORS IN RUBIDIUM VAPOR

In this experiment, we used rubidium as a resonant absorber for the generation of optical precursors. Production of a sharp rising edge or trailing edge is crucial for the generation of optical precursors. With the development of femtosecond laser and pulse shaping techniques, pulses with tens of femtosecond even sub-10 fs rising edge and trailing edge can be obtained easily and pulses with customized shapes can be obtained out of the short laser pulses. Specifically, in our experiment, dazzler was used as the pulse shaper to produce pulses with sharp rising and trailing edges. Dazzler is a commercialized acousto-optic programmable dispersive filter (AOPDF). Dazzler can in principle take the place of any linear optical instruments. The pulse shaping window of the dazzler used in this experiment is about 7 picoseconds. In our experiment, we shaped 40 fs amplified pulse to a 7-ps square pulse with center wavelength coinciding with Rb D1 absorption line at 794.6nm by dazzler. Then we sent this square pulse into rubidium cell and measured the output pulse shape with a streak camera with 2-ps resolution.

2.1 Experiment setup

The experiment setup is shown in Fig. 1. The femtosecond amplifier system produces 40 fs pulses with pulse energy of 1 mJ. Limited by the damage threshold of dazzler, we cannot apply more than 30mW input power on the dazzler. The dazzler shapes pulses in time domain. The pulse shaping window is 7ps in our case. The maximum efficiency that can be transformed from input pulse to out pulse is about 50%

for each frequency component. The spectral resolution of dazzler is about 1nm. The pulses from amplifier, after being attenuated, are sent to dazzler. Dazzler will shape the pulse from a 40fs pulse to a 7-ps square pulse. We also let dazzler choose the center frequency of the square pulse to coincide with Rb D1 line 794.6 nm. Therefore after square pulses are sent to the rubidium cell the center frequency components are absorbed and dispersion is added to other frequency components. The absorbance of the rubidium vapor can be controlled by controlling the temperature of the cell. We heated it gradually to 202 Celsius to achieve an atom number density about $10^{15}/cm^3$. The pulses propagating out of Rb cell was then measured by a streak camera with 2-ps resolution.

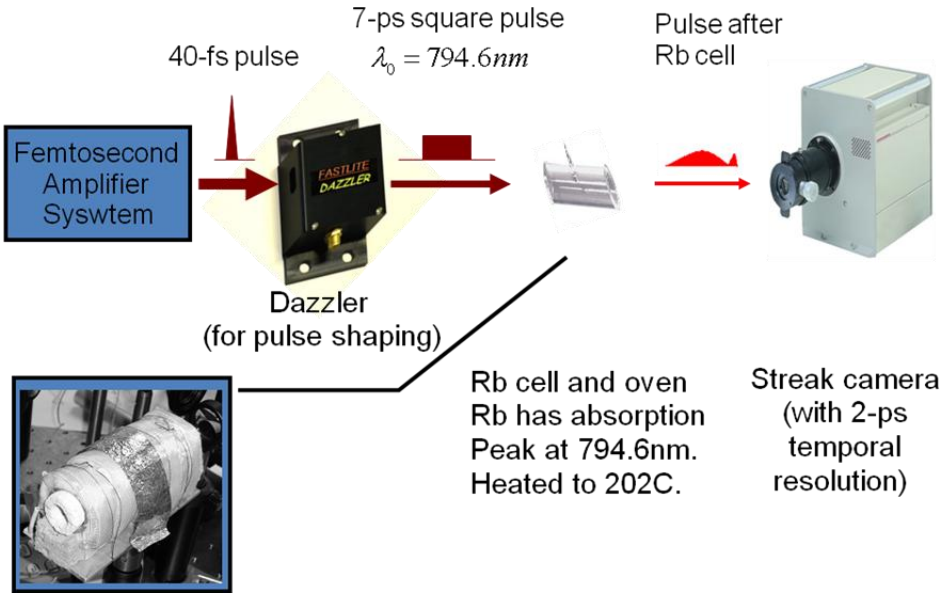

Fig. 1. Experiment scheme for observing optical precursors in rubidium vapor. 40 fs optical pulses produced by a Coherent femtosecond amplifier system are fed into dazzler. Dazzler produces square pulses about 7 picoseconds long. The square pulses also have center wavelength coincide with the Rb D1 line 794.6nm. These square pulses are sent to a rubidium cell which is heated gradually to around 202 C. Then the output pulses are measured by a streak camera with 2-ps resolution.

Pulse shaping

Pulse shaping was carried out by dazzler. To obtain the desired pulse shape we need to measure the spectrum of the input 40fs pulse $E_0(\nu)$ first. Then we calculated the desired spectrum for 7ps square pulse $E_{sq}(\nu)$. Dazzler was then used as a linear filter to transform $E_0(\nu)$ to $E_{sq}(\nu)$ by apply this filter term $A(\nu) = E_{sq}(\nu) / E_0(\nu)$ to the input pulse $A(\nu) = E_{sq}(\nu) / E(\nu)$. During this process, we assume the input pulse is transform limited. In fact, by using frequency resolved optical gating (FROG) or other measurement techniques, it is possible to measure the phase of the input pulse. However, to assume the pulse from the amplifier a transform limited pulse is a good approximation.

Prepare the rubidium vapor

The rubidium cell needs to be heated up and cooled down slowly. It takes one hour or so for Rb vapor to reach thermal equilibrium with the heater. In this experiment, the rising or lowering of the temperature are done in steps: 202C (12.75V), 182C (12V), 147C (10V), 101C (8V), 68C (6V). The number following the temperature was the voltage used for the heater.

2.2 Experiment results

By changing the temperature from about 50C to 202C, we measured the change of pulse shapes after transmitting though Rb vapor, which are shown in Fig. 2.

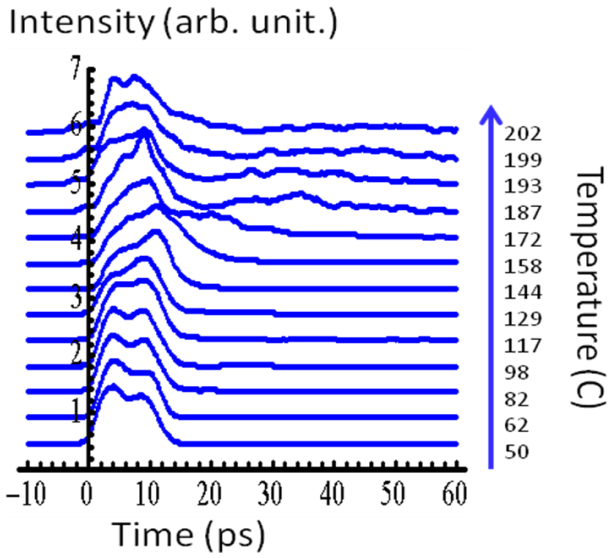

Fig. 2. Measured pulse shapes transmited throught Rb vapor with different temperatures. The intensities are rescaled. Time zero is the starting point for the pulse.

From Fig. 2. we can see that, as the temperature rose, the absorption became stronger and there was a so-called main pulse seperated from the original pulse.The main pulse was delayed compared with the pulse front. The pulse front showed optical precursor behavior and showed little delay, see Fig. 3 for example.

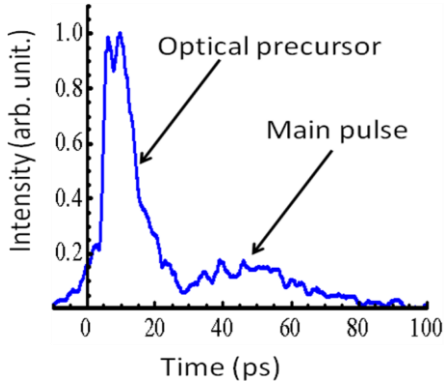

Fig. 3. Optical precursor and the delayed main pulse.

2.3 Theory for optical precursors in rubidium vapor

Optical precursor is a linear effect. When center spectrum of a pulse with sharp edge is absorbed by an absorber, dispersion, which come with the absorption, will cause change of group velocity. So, the group velocity of frequency around the absorption center should be largely lower than speed of light in vacuum. This part of spectrum forms the so-called main pulse. The frequency components far from frequency center experience negligible dispersion, therefore, are not delayed and form an optical precursor. There should be some frequency with group velocity bigger than speed of light in vacuum; however Kramers-Kronig relation guarantees the causality, so nothing will go faster than speed of light in vacuum. To simulate this process with rubidium vapor as absorber and the 7 ps square pulse as input pulse, we did the following calculation.

The spectral amplitude and phase of a 7-ps square pulse $E_{sq}(\nu)$ can be calculated. When such a pulse is sent through rubidium vapor, and absorbed the central part of the spectrum is absorbed. The absorption line of rubidium vapor is mainly Doppler broadened and has a Gaussian shape absorption line. The cross section can be calculated [19] from the spontaneous decay rate for D1 line $\lambda \simeq 794.8nm$

$A = 1/t_{sp} = 3.81\times10^{7}\, rad\cdot Hz$, where t_{sp} is spontaneous life time [20, 21].

$$\sigma(\nu) = \frac{\lambda^2}{8\pi t_{sp}} g(\nu), \qquad (1)$$

t_{sp}, λ is center wavelength, and $g(\nu)$ is the normalized line shape. After considering the collision broadening about 61 radMHz [22], the line shape is defined by Lorentzian line shape $g_{col}(\nu)$. For Doppler broadened medium, the line shape will become

$$\bar{g}(\nu) = \int_{-\infty}^{\infty} g_{col}\left(\nu - \nu_0 \frac{\mathrm{v}}{c}\right) p(\mathrm{v}) d\mathrm{v}, \tag{2}$$

where

$$p(\mathrm{v}) = \frac{1}{\sqrt{2\pi}\sigma_{\mathrm{v}}} \exp\left(-\frac{\mathrm{v}^2}{2\sigma_{\mathrm{v}}^2}\right), \text{ with } \sigma_{\mathrm{v}}^2 = kT/M, \tag{3}$$

where T is the temperature of the gas, M is the mass of the Rb atom. The total absorption is defined

$$\frac{E_{out}(\nu)}{E_{sq}(\nu)} = \exp[-n(T)L\sigma(\nu)], \tag{4}$$

where n(T) is the Rb atom number density which depends on temperature T and L is the length of the cell. It is strait forward to calculate $E_{out}(\nu)$. By making inverse Fourier transform, the electric field in time domain can be obtained and therefore can be compared with experiment results.

The calculated results are show in Fig. 4.

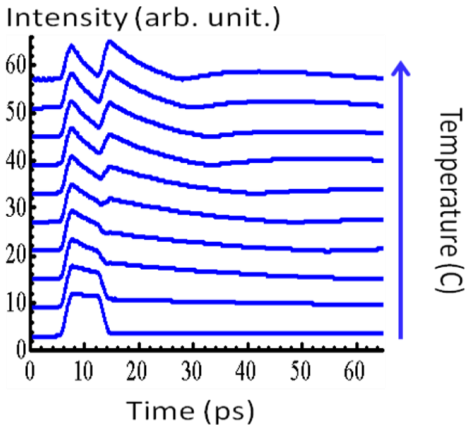

Fig. 4. Theoretical calculated pulse shapes after a 7-ps square pulse transmitted through a rubidium cell with different temperatures.

2.4 Comparison of experiment results and theory

At low temperature, the absorption of Rb vapor is weak and therefore the pulse is not distorted at all. The character of resultant pulse shape for this temperature range is that there is no deformation of pulse shape compared with original pulse. We can say it has no tail, which is a term used to compare with pulse shapes at high temperature. Please see Fig. 5 for illustration.

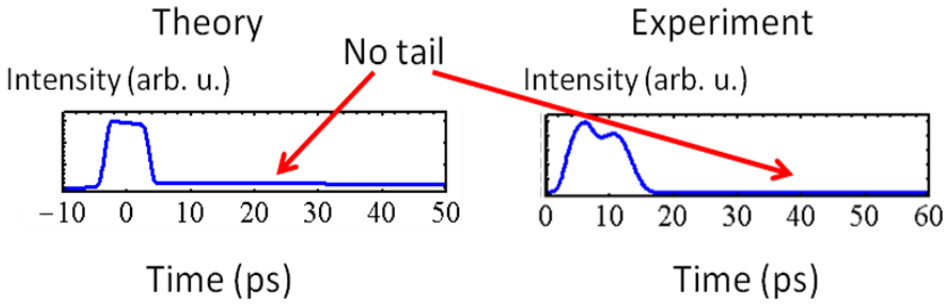

Fig. 5. Comparison between theory and experiment for lower temperature. The pulse shape is not changed.

As temperature goes up, input pulses are absorbed more by Rb vapor and dispersion from Rb upon input pulses is also stronger. As a result, tail pulse shows up right after the original pulse, please see Fig. 6.

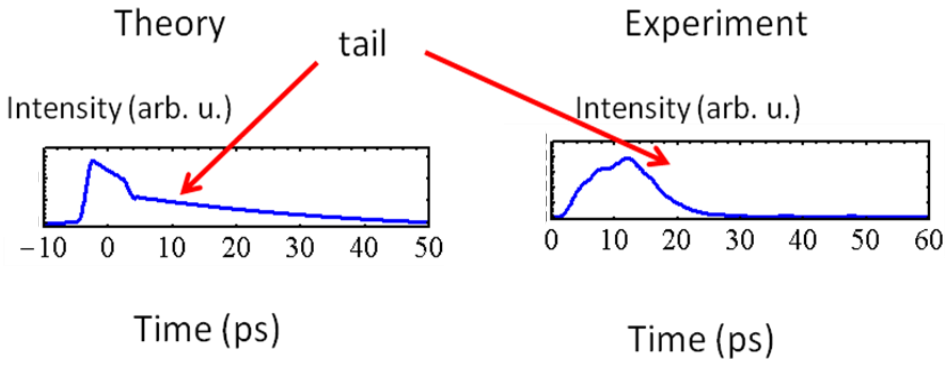

Fig. 6. Comparison between theory and experiment for higher temperature. The characteristic tail shows up right after the original pulse.

As temperature goes very high, the center spectrum of input pulse are all absorbed by Rb vapor and the corresponding dispersion split the input pulse into the pulse front and a so-called main pulse, please see Fig. 7. The pulse front, which shows little delay, is optical precursor.

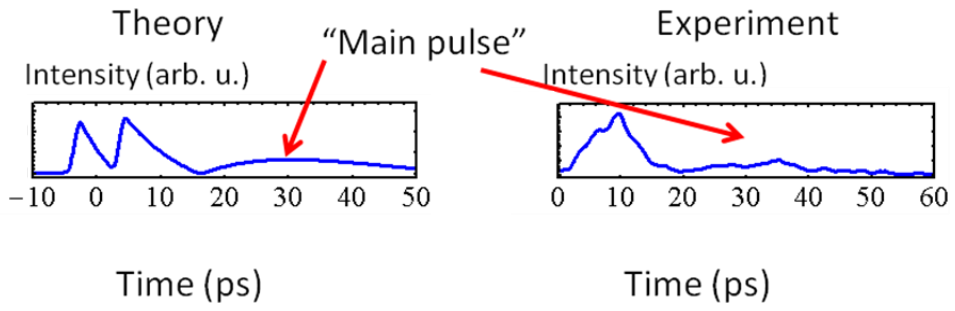

Fig. 7. Comparison between theory and experiment for very high temperature. A so-called main pulse is separated from the pulse front, which is called optical precursor.

At even higher temperater, the main pulse is not only delayed more but also attenuated strongly. The optical precursor shows a much less attenuation. It is another property of optical precursor and also a reason why people want to use optical precursor in optical communications.

2.5 Summary

In the experiment, by increasing the temperature of Rb vapor and therefore the number density of Rb vapor, we observed the progression of the formation of optical precursors. The pulse shapes at each stage of the formation of optical precursors showed traits that are well explained by theory.

3. SUPERRADIANCE AND ITS RELATION WITH OPTICAL PRECURSORS

Superradiance was first theoretically predicted by Dicke [11]. The main idea is that if a group of atoms are very close to each other and the electric field experienced by them can be regarded as equal, they can be considered as a whole instead of individual particles. As a result, they emit lights in the way that emitted electric fields are added up constructively. So electric field is proportional to number of atoms N and therefore the intensity of the radiation depends on N^2. Also due to the energy conservation, the emission duration is shortened by N^2 times.

Superradiance in large sample is a very complicated process [13]. In this part, we will show that solving Maxwell-Bloch equations can explain some of the results in the 3-photon excited superradiance experiment in Rb vapor in low excitation regime carried out in our lab by Ariunbold. We will show that the superradiance can be understood by the generation of pulse with sharp rising edge and the propagation of this pulse through a resonant medium. Therefore, the superradiance in the low excitation regime can be understood as an optical precursor phenomenon.

3.1 Experiment scheme

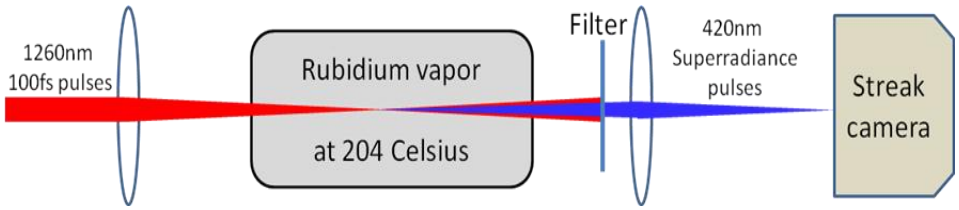

Fig. 8. Scheme for 3-photon excited superradiance experiment of Aribunbold.

Fig. 8 shows the experiment scheme of the experiment carried out by Ariunbold[18]. The rubidium vapor was pumped by 1250nm 100 fs pulses with 3-photon excitation. Then the generated superradiance pulses were measured by a streak camera with 2ps temporal resolution. The excitation of rubidium vapor was a 3-photon process. So we assume the excitation only occured in the focal volume in the cell. Therefore, it will be shown that the superradiance is naturally treated in two steps, the first step is the generation of pulse in the focal volume and the second step is the propagation of this pulse through the rest of the medium. The measurement of superradiance pulses by streak camera are taken into account later as the last step of the simulation.

3.2 Weak excitation limit

In Ariunbold's experiment, the excitation by femtosecond laser was weak. This is because the excitation process was a 3-photon process and the input laser's power was low (1mW to 3mW).

Take 1mW for example, we can show the excitation rate for rubidium vapor is low. The repetition rate of the laser is 1kHz. So the pulse energy is 1μJ. We assume the pulse is a $\tau = 100\,fs$ square pulse with beam radius 8 μm in the focal volume. The volume of the pulse is $V = \pi(8\mu m)^2(100\,fs \times c)$, where c is the speed of light in vacuum. The electric field can be calculated from pulse energy $Energy = \varepsilon_0 E^2 V$. We got $E = 6.1\times10^9 V/m$. The Rabi frequency is $\Omega = \mathrm{E}\mu/\hbar,$ where μ is the dipole moment $\mu = e\left|\langle b|\vec{r}|a\rangle\right|$, $|a\rangle$ and $|b\rangle$ are levels of the two level system. From the spontaneous life time, we can estimate the value of dipole moment $\mu = \sqrt{3\varepsilon_0 hc^3/(2t_{sp}\omega^3)} = 2.2\times10^{-30} C\cdot m$. Here the ω is the angular frequency of 1260nm light. Since, it is 3-photon process, the 3-photon Rabi frequency is $\Omega_{3ph} = \Omega^3/(2\omega)^2$. The probability of excitation is $\sin(\Omega_{3ph}\tau) = 0.04$. This shows that we are at very low excitation regime. As a result, there is no delay between generated superradiance pulse and pump pulse.

3.3 Available theories

In this thesis, we only consider the superradiance of two level atoms. For two-level systems, Dicke's model [11] gave pretty accurate solutions in samples much shorter than wavelength. For larger samples, it is necessary to solve Maxwell-Bloch equations (MBE) [23]. In this research, we use Maxwell-Bloch equations, because they can reproduce Dicke's model for small samples and also works for larger samples. By using MBE, we don't have to worry about the validity of using Dicke's model.

3.4 Strategy of simulation

The simulation is divided into three parts. In the first part, the Maxwell-Bloch equations take the following form:

$$\begin{cases} \partial_t \rho_{aa}(z,t) = -2\left[\Omega(z,t) + \Omega_3(z,t)\left(r(z)/r_0\right)^3\right]\rho_{ab}(z,t) \\ \partial_t \rho_{bb}(z,t) = 2\left[\Omega(z,t) + \Omega_3(z,t)\left(r(z)/r_0\right)^3\right]\rho_{ab}(z,t) \\ \partial_t \rho_{ab}(z,t) = -\gamma\rho_{ab}(z,t) + \left[\Omega(z,t) + \Omega_3(z,t)\left(r(z)/r_0\right)^3\right]\left[\rho_{aa}(z,t) - \rho_{bb}(z,t)\right] \\ \partial_z \Omega(z,t) + \left(1/c\right)\partial_t \Omega(z,t) = \eta\rho_{ab}(z,t) \\ \partial_z \Omega_3(z,t) + \left(1/c\right)\partial_t \Omega_3(z,t) = 0, \end{cases} \quad (5)$$

where $\eta = \left(1/t_{sp}\right)3N(T)\lambda^2/\left(8\pi\right)$ and $N(T)$ is the density of particles, which depends on temnperature T .The $\Omega_3\left(z,t\right)$ is the Rabi frequency induced by 1260nm pump light and $\Omega\left(z,t\right)$ is the 420nm emitted by the rubidium atoms. The initial condition is $\Omega_3(z_0,t) = \left[\frac{\mu}{\hbar}E_0(t)\right]^3/\left(2\omega_0\right)^2$, $\Omega_3(z,t_0) = 0$, $\rho_{bb} = 1$ and all other components are zero at t_0 and z_0 which is initial time and boundary. The $r\left(z\right)$ is the beam radius at a particular position, and is calculated according to Gaussian beam geometry. r_0 is the beam radius at the focal point. In the simulation, the time t is from 0 to 200ps. The z is from 0 to 1mm.

The second part of the simulation is the propagation of 420nm pulse, which is generated from the first part of the simulation, through the rest of the rubidium cell. The Maxwell-Bloch equations are as below:

$$\begin{cases} \partial_t \rho_{aa}(z,t) = -2\Omega(z,t)\rho_{ab}(z,t) \\ \partial_t \rho_{bb}(z,t) = 2\Omega(z,t)\rho_{ab}(z,t) \\ \partial_t \rho_{ab}(z,t) = -\gamma\rho_{ab}(z,t) + \Omega(z,t)\left[\rho_{aa}(z,t) - \rho_{bb}(z,t)\right] \\ \partial_z \Omega(z,t) + (1/c)\partial_t \Omega(z,t) = \eta\rho_{ab}(z,t). \end{cases} \quad (6)$$

The simulation length for z is 0 to around 25mm.

The third part of the simulation is to take the measurement by streak camera into consideration. The streak camera has a temporal resolution of 2ps and the data processing process used averaging too. All these are taken into account in this part.

3.5 Solving MBE with Mathematica 8

In this research, we use commercial software Mathematica 8 to solve the MBE. Mathematica provides a command called NDSolve to solve differential equations numerically. However, it is not straight forward to do so. The computer I used has limited memory (4GB) and this has proved to be the biggest limitation in this research. The parameters of the command have to be well chosen. The command NDSolve has a small sweet area in the parameter space, in which the software will give good enough results. With parameters outside of this sweet area, either the accuracy is so poor that the results are noisy or the computer get overload and quit the software.

The order of the variables in the equation is important. In the simulation we always define the function with variable z before t. In this way, the NDSolve command will cut z into steps and evaluate the function at the whole range of t in each step of z and proceed to the next value of z. This is particularly suitable to our simulation because

we are trying to find out the electric field at a particular position (end) of the sample, i.e. a certain value of z.

The parameters I encountered in the simulations are StartingStepSize, MaxStepSize, MaxSteps, Method, AccuracyGoal, and PrecisionGoal. The basic rule is if the software produces meaningful and good looking results, then there is no need to use any of the above parameters. When I don't designate these parameters, the software will choose these parameters depending on the form of differential equations, range of variables for evaluation and initial & boundary conditions. However, sometimes, these computer chosen parameters yield poor results and, in this research, the computer produces poor results almost every time. Therefore, I have to define the parameters on my own. I do not use all of them each time. Instead, I try to specify the least amount of parameters. That is because firstly the software is very smart and will do the right thing if given a little hint; secondly parameters sometimes are conflict with each other and may further complicate the calculation.

Now I will talk about my impression of each parameter with the example of our simulation of MBE. Though the descriptions of parameters are available in the help page of Mathematica, I found them not quite clear to me until I get my own feeling about them by using them.

StartingStepSize defines the initial step sizes of parameters. The beginning of the simulation is extremely important in general. A small error in the beginning could cause big error in the end. Therefore, it is necessary to use smaller steps in the beginning to get more precise results. In our case, it is especially necessary because the initial excited

atoms are localized in the short length of the beginning of the sample see Fig. 9. Therefore, in that small section, a sharp rising edge of electric field will be produced, so the initial step of time should be smaller than the rising time of the produced pulse and the initial step of length z should be able to resolve the variations of degree of excitation in the section of excited atoms. (Fig. 9 is just an example. Not every calculation uses this configuration.)

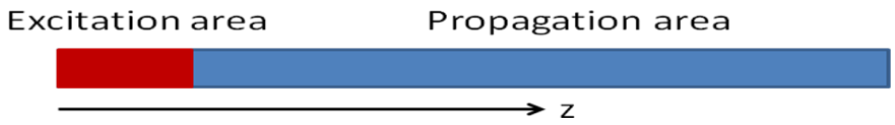

Fig. 9. Two parts of the simulation of superadiance.

PrecisionGoal and AccuracyGoal define the required precision and accuracy for final result. They will in turn limit the precision or accuracy of each step of calculation. When I got some results without using these two parameters, I will set them to the order of the result I got. For example, if I got $\Omega(z,t)$ of the order of 10^{-7}, then I will set PrecisionGoal and(/or) AccuracyGoal to 7 maybe 8 and run the command again, so that I can see whether this result changes due to this requirement of precision and accuracy. In such a way, I can find a reliable result. Too big AccuracyGoal may cause problems, because the initial condition may not achieve that accuracy, and the software will stagnate at the first several steps and you will have to stop the software manually. PrecisionGoals sometimes will not affect the results much even if you set it to 100. So in our simulation AccuracyGoal is more useful.

MaxStepSize is useful because sometimes you will get wrong results without limiting the step size, some small but important features of initial and boundary condition maybe neglected by the software if the step size is too big. I felt that, when the precision goal and accuracy goal is met the software will tend to use big step sizes. Therefore, it is important to limit the max step size. In our case, we have two parameters z and t. Since we write functions like $\Omega(z,t)$, when defining the step size, it should be written like MaxStepSize $\rightarrow \{0.00001, 0.1\}$, which means the 0.00001 is the maximum step size along z direction and 0.1 is the maximum step size for t. When both StartingStepSize and MaxStepSize are used, I don't know when, where and how the step sizes are changed to MaxStepSize.

MaxSteps will limit the total steps used in the calculation. It is especially useful when the software tends to stagnate. With such a limitation, the software will stop automatically when it stagnates, so that we got a chance to change parameters and restart the calculation. If MaxSteps is not defined to a proper value, the software may fill the computer memory when it stagnates, you may experience difficulty to stop the software without turning off power of the computer. However, if the calculation is big and the default number of MaxSteps is too small, you can set it to infinity so that the software will not stop in the middle of the calculation.

Method is the last parameter to try if nothing above provides good results. I used "BDF", "Adams" and "MethodOfLines" sometimes, and they produce better results than without designating the methods in tough situations.

3.6 Results of simulation and its comparison with experiments

In the simulation, we started from the experiment parameters used in Ariunbold's experiment. Then we varied the parameters and see how they affect the final results. The experiment use 100fs pulse as pump pulse. The Rayleigh length of the focal volume is about 100 micron. The laser power is from 1mW to 3mW with repetition rate 1 kHz. The length of the cell is about 2 inches. The focal point is near the center. So the propagation length after the focal volume is about 23mm. The resolution of streak camera is 2ps and the moving average 20 (, which is a duration about 7ps,) is used to get the final pulse shape. The following results were obtained by varying only one of the above parameters and keeping other parameters same.

The pulse shape obtained in the first part of simulation with different pulse duration (FWHM) of the pump laser is shown in Fig. 10.

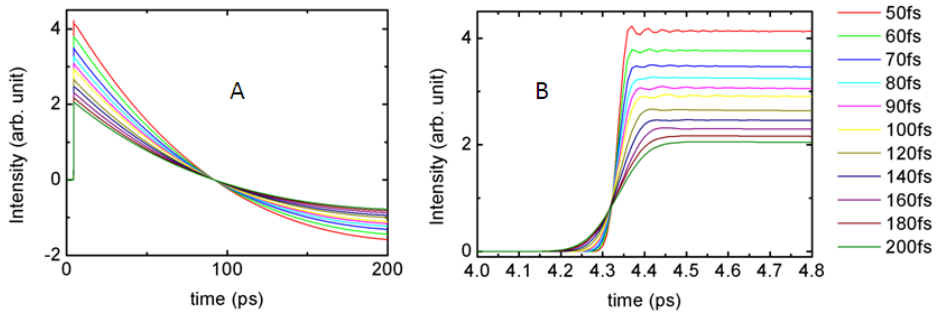

Fig. 10. Pulse shapes obtained from the first part of the simulation with different pump laser pulse durations.

From Fig. 10 B, we can see that the longer duration the pump laser is the less sharper the generated pulse. In the experiment, 100fs pulses are used. So the front edge

is pretty sharp compared with the trailing edge of the generated pulse (Fig. 10 A). After these pulses propagated through the rest of the cell and measured by streak camera, we can get the final pulse shapes in Fig. 11.

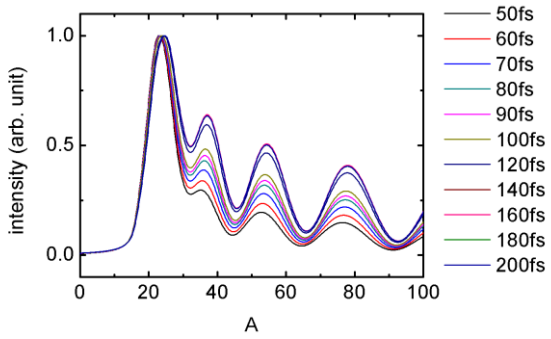

Fig. 11. Final pulse shapes with pump lasers of different pulse durations.

Fig. 12 shows the final pulse shape due to different propagation length after the focal volume. We can see that the longer propagation length the closer the peaks are.

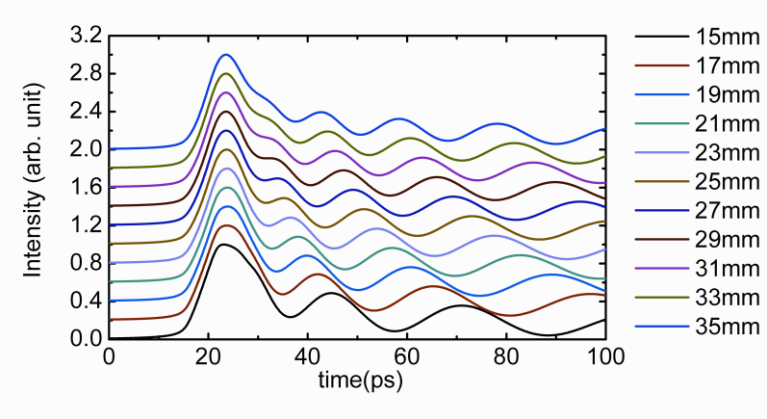

Fig. 12. Final pulse shapes for different propagation lengths after the focal volume.

Fig. 13 shows the final pulse shape for different powers of pump laser.

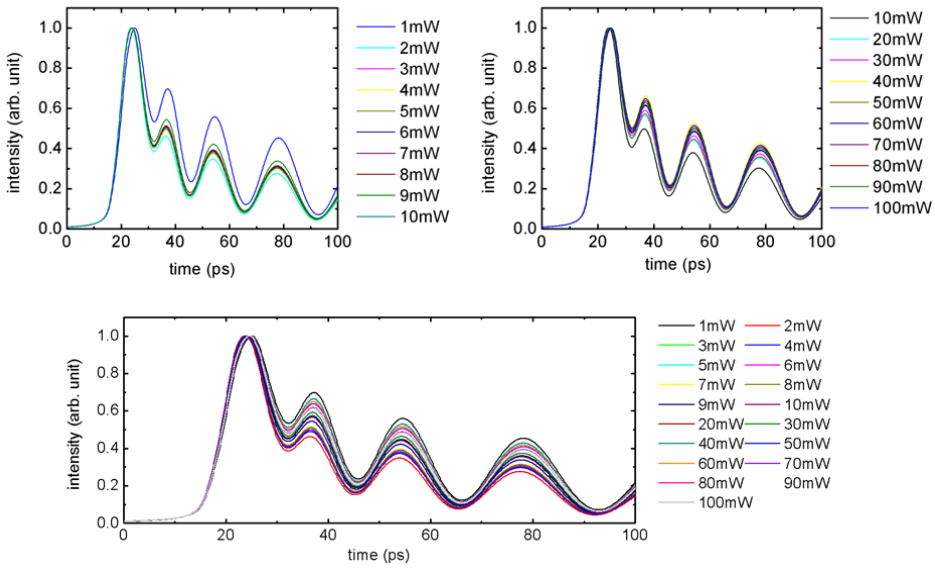

Fig. 13. Final pulse shapes for different pump laser powers.

Different pump power will make change the relative heights of the peaks in the final pulse shape. However, the relative height of peaks changes irregularly due to the change of power. Therefore, these changes might be merely an artifact due to the error in the simulation.

Fig. 14 shows the pulse shapes obtained by varying Rayleigh length of the pump laser in the first part of the simulation.

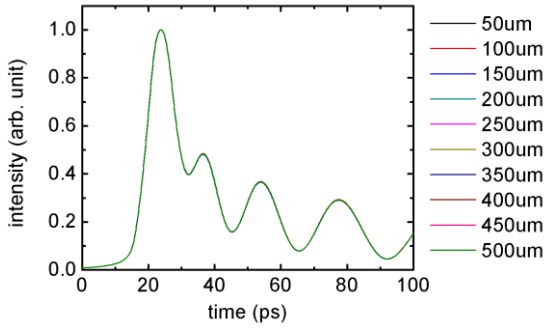

Fig. 14. Final pulse shapes for different Rayleigh lengths of the pump laser in the first part of simulation.

We can see from Fig. 14 that the Rayleigh length does not change the final pulse shape at all, which is a little suprising.

Fig. 15. shows the final pulse shape due to different moving average value in the last step of simulation, which simulate the data processing process in the experiment.

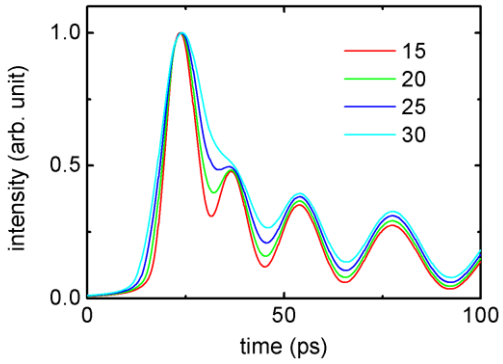

Fig. 15. Final pulse shapes for different moving average values.

We can fit the experiment results with the above simulation values by changing the length of propagation after the focal volume. The result is shown in Fig. 16.

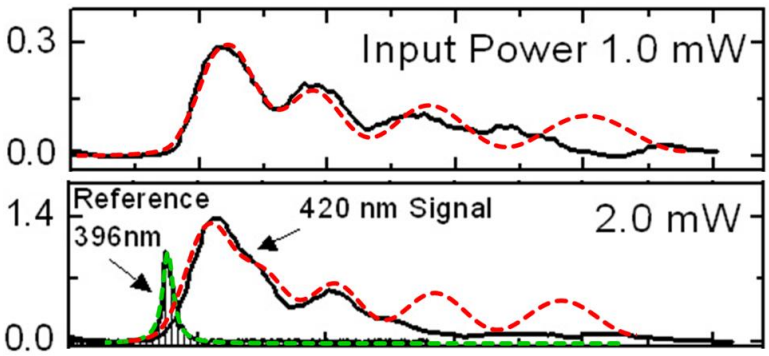

Fig. 16. Theoretical fitting for the experimentally measured pulse shapes. The dotted lines are theoretical calculated pulse shapes. The solid lines are Ariunbold's experiment data[18]. For 1mW result, the propagation length in the simulation is 21 mm. For 2mW result, the propagation length in the simulation is 35 mm. The green dotted line fitted the reference pulse well. The moving average used here is 20. The pump pulse duration is 120fs. Rayleigh length is 100 micron.

Fig. 16 shows that the theory can fit one of the experiment data. However, the change of propagation length is not explained in this theory. It could be cause by some nonlinear process like self-focusing.

Fig. 10 shows that the pulse generated in the focal volume is a pulse with sharp rising edge and a long trailing edge. Such a pulse after transmitted through a resonant medium will show precursor behavior, which looks like a pulse with ringing. Fig. 10 shows that as the pump laser get longer, the rising edge get less sharp. It could be imagined that as the pump laser become very long, the superradiance can no longer be understood as a optical precursor formation process.

3.7 Summary

We have conducted a numerical simulation to explain the 3-photon excited superradiance experiment in Rb vapor conducted by Ariunbold. In the simulation, we solved Maxwell-Bloch equations numerically with Mathematica 8. The experiment result with certain pump power can be well fit by the simulation with proper choice of propagation length of superradiance pulse in Rb vapor.

The simulation demonstrated the relation between optical precursors and the superradiance in the above setting. The pulses generated in the first (generation) part of the superradiance simulation has very sharp pulse front (Fig. 10). It then propagates through the resonant medium Rb vapor. Such configuration fit perfectly with the setup of generating optical precursors. The resultant pulse shapes in Fig. 11-16 show ringing, which are the characters of optical precursors. The power of pump laser was low which means atoms are weakly excited so that no delay show up between pump pulse and superradiance pulse. So we claim the 3-photon excited superradiance generated by a femtosecond pump pulse at low excitation regime can be understood as a process of generation of optical precursors.

4. CONCLUSIONS

In this thesis, we shaped 40 femtosecond pulses to 7-ps square pulses with center frequency on resonant with Rb D1 line at 794.8nm. After passing these square pulses through a hot Rb cell we observed optical precursors in a fast streak camera. The progression of formation of optical precursors was demonstrated by varying the temperature of the rubidium cell. The experiment results were well explained by theory. We also solved Maxwell-Bloch equations numerically with Mathematica 8 to simulate the 3-photon excited superradiance in Rb vapor in low excitation regime. Thus, we showed that 3-photon excited superradiance that was pumped by femtosecond pump pulses in low excitation regime can be understood as the formation of optical precursors. The experiment results for a certain pump power were matched by the theory with different choice of propagation lengths.

REFERENCES

1. A. Sommerfeld, "Über die fortpflanzung des lichtes in dispergierenden medien," Ann. Phys. (N.Y.) **44**, 199 (1914).
2. L. Brillouin, "Uber die fortpflanzung des licht in disperdierenden medien," Ann. Phys. (N.Y.) **44**, 204 (1914).
3. L. Brillouin, *Wave Propagation and Group Velocity* (Academic Press, New York, 1960).
4. S. H. Choi, and U. Osterberg, "Observation of optical precursors in water," Phys Rev Lett **92**, - (2004).
5. J. Aaviksoo, J. Kuhl, and K. Ploog, "Observation of optical precursors at pulse-propagation in GaAs," Phys Rev A **44**, R5353-R5356 (1991).
6. H. Jeong, A. M. C. Dawes, and D. J. Gauthier, "Direct observation of optical precursors in a region of anomalous dispersion," Phys Rev Lett **96**, - (2006).
7. S. W. Du, C. Belthangady, P. Kolchin, G. Y. Yin, and S. E. Harris, "Observation of optical precursors at the biphoton level," Optics Letters **33**, 2149-2151 (2008).
8. D. Wei, J. F. Chen, M. M. T. Loy, G. K. L. Wong, and S. W. Du, "Optical precursors with electromagnetically induced transparency in cold atoms," Phys Rev Lett **103**, - (2009).
9. A. V. Sokolov, L. M. Naveira, M. P. Poudel, J. Strohaber, C. S. Trendafilova, W. C. Buck, J. Wang, B. D. Strycker, C. Wang, and H. Schuessler, "Propagation of ultrashort laser pulses in water: linear absorption and onset of nonlinear spectral transformation," Appl Optics **49**, 513-519 (2010).

10. M. M. Springer, W. Yang, A. A. Kolomenski, H. A. Schuessler, J. Strohaber, G. W. Kattawar, and A. V. Sokolov, "Observation of precursorlike behavior of femtosecond pulses in a dye with a strong absorption band," Phys Rev A **83**, 043817 (2011).

11. R. H. Dicke, "Coherence in spontaneous radiation processes," Phys Rev **93**, 99 (1954).

12. C. Stroud Jr, J. Eberly, W. Lama, and L. Mandel, "Superradiant effects in systems of two-level atoms," Phys Rev A **5**, 1094-1104 (1972).

13. M. Gross, and S. Haroche, "Superradiance: an essay on the theory of collective spontaneous emission," Physics Reports **93**, 301-396 (1982).

14. L. Allen, and J. H. Eberly, *Optical Resonance and Two-Level Atoms* (Dover publications, Mineola, NY, 1987).

15. M. Gross, C. Fabre, P. Pillet, and S. Haroche, "Observation of near-infrared dicke superradiance on cascading transitions in atomic sodium," Phys Rev Lett **36**, 1035 (1976).

16. N. Skribanowitz, I. P. Herman, J. C. MacGillivray, and M. S. Feld, "Observation of dicke superradiance in optically pumped HF gas," Phys Rev Lett **30**, 309 (1973).

17. G. O. Ariunbold, M. M. Kash, V. A. Sautenkov, H. Li, Y. V. Rostovtsev, G. R. Welch, and M. O. Scully, "Observation of picosecond superfluorescent pulses in rubidium atomic vapor pumped by 100-fs laser pulses," Phys Rev A **82**, 43421 (2010).

18. G. O. Ariunbold, W. Yang, A. V. Sokolov, V. A. Sautenkov, and M. O. Scully, "Picosecond superradiance in three-photon resonant medium," (To be submitted to Phys. Rev. A) (2011).

19. B. E. A. Saleh, and M. C. Teich, *Fundamentals of Photonics* (Wiley Interscience, Hoboken, N.J., 2007).

20. J. Sansonetti, "Wavelengths, transition probabilities, and energy levels for the spectra of rubidium (Rb I through Rb XXXVII)," Journal of Physical and Chemical Reference Data **35**, 301-421 (2006).

21. P. Siddons, C. S. Adams, C. Ge, and I. G. Hughes, "Absolute absorption on rubidium D lines: comparison between theory and experiment," Journal of Physics B: Atomic, Molecular and Optical Physics **41**, 155004 (2008).

22. C. S. Yi, "Pressure effects of homogeneous rubidium vapour on its resonance lines," Phys Rev **58**, 884-887 (1940).

23. J. C. MacGillivray, and M. Feld, "Theory of superradiance in an extended, optically thick medium," Phys Rev A **14**, 1169-1189 (1976).

VITA

Name: Wenlong Yang

Address: Department of Physics and Astronomy, Texas A&M University, College Station, TX, 77843-4242.

Email: ywlonion@hotmail.com

Education: B. S. Physics, Nankai University, 2005

M. S. Theoretical Physics, Chern Institute of Mathematics, Nankai University, 2008

M. S. Physics, Texas A&M University, 2011